Prediction of Bending Limits in Friction-Stir-Processed Thick Plate Aluminum

M.P. MILES, M.W. MAHONEY, and C.B. FULLER

Friction-stir processing (FSP) was used to modify surface microstructures, to enhance the bending of thick-plate 6061-T6 and 7050-T7451 aluminum alloys. Plates were bent at room temperature into a V-shaped die, to various angles. Bending performance in the friction-stir-processed plates was significantly better than that in the base plates, where processing caused localized softening of the pretensile surface of the plate. A finite-element model of the plate-bending process was developed, to predict the bending limits of both the unprocessed base plates and of the friction-stir-processed plates. For the friction-stir-processed plates, the model employed a mesh divided into two or more zones; one zone was for unprocessed base material and other zones were for the processed material or for material that was affected by the heat of processing. The model used both the von Mises and the Latham and Cockroft criteria to predict bending limits. The bending-limit predictions were reasonably accurate, provided the gradient in true stress-strain behavior through the plate thickness was well characterized.

I. INTRODUCTION

THE bending of thick metal plates, defined as greater than about 12 mm in thickness, is typically governed by the bend radius and the ductility of the material. A thick 6061-T6 aluminum plate is difficult to bend to any significant degree, because of its high strength and its relatively low ductility, as measured by its total elongation in a tensile test. However, the advantages to bending thick plates include the resulting structural properties, which are better than welded structures, and the reduced fabrication costs. Plates bent to the proper shape avoid the degradation in properties that accompanies welding.

One new method that can be used to increase the bending limits of thick plates is friction-stir processing (FSP). The FSP method is a variation of traditional friction-stir welding (FSW), but in this case, it can be used to locally modify the properties in a part.[1–9] The effect of processing the pretensile surface of a heat-treatable aluminum-alloy plate is to locally anneal and refine the grains in the material. This increases the surface ductility to a depth equivalent to the FSP penetration and significantly enhances its bending limit. This ductility increase can be attributed to both the refined and more homogeneous microstructure and to the annealed condition of the surface material. The separate contribution of each has not been determined. This would be a worthwhile exercise, but it is beyond the scope of the research reported in this article. However, in a separate research effort, attempts were made to create an annealed surface in an aluminum plate by rapid, localized induction heating. Frequencies were adjusted to provide shallow, skin-depth heating.[10] Further, the goal was to minimize the loss of strength in the remainder of the plate, by rapid extraction of heat from the opposite side. This would have provided an annealed surface without the severe deformation associated with FSP, which leads to the recrystallization and the fine microstructure. Unfortunately, due to the very high thermal conductivity of aluminum alloys, it was not possible to anneal a reasonable depth of material (at least 3-mm deep) without excessively overaging the remainder of the plate. Regardless of the rates of heating and cooling, a static thermal loading eventually resulted in a steady-state temperature profile, which caused softening to a much greater degree than was desired. Similar results were obtained using transient temperature profiles, *i.e.*, induction power was cycled per a predetermined theoretical best-condition cycle. Based on these experiments, it does not appear that conventional heating approaches can selectively anneal thick aluminum plate without significantly reducing mechanical properties in the remainder of the plate.

The promise of using FSP as a method of tailoring material properties locally in a part leads us to develop a predictive model that will allow us to evaluate the effect of processing on bending performance. Most of the simulation work done thus far on FSW and processing has focused on the process itself. One of the first predictions of the thermal profile that occurs during FSW was based on the Rosenthal equation[11] and on models that assumed that the tool had a moving heat source.[12,13,14] These approaches simplified the problem by using an analytical model to calculate the heat input from friction and deformation. Finite-element methods have been used to model heat transfer and to understand material flow,[15] especially in steady-state conditions, using either an Eulerian approach or an Arbitrary Lagrangian Eulerian (ALE) approach, in which the material is modeled as a viscous fluid.[16,17] This last approach provides information about material flow, both allowing for the evaluation of different tooling designs and permitting a temperature calculation based on material deformation.

In the current work, the modeling effort is not focused on the processing, but on the prediction of the bending performance of a processed plate. Therefore, the mechanical properties of the plate were not predicted by the model, but were determined experimentally by tension testing. These properties were then used as inputs to a finite-element model and were coupled with failure criteria, in order to estimate the bending limits of friction-stir-processed plates. Model predictions were compared

M.P. MILES, Assistant Professor, is with the Manufacturing Engineering Technology Department, Brigham Young University. Contact e-mail: mmiles@byu.edu M.W. MAHONEY and C.B. FULLER, Scientists, are with Rockwell Scientific Company.

Manuscript submitted February 4, 2005.

to bending experiments on thick plates of aluminum alloys 6061-T6 and 7050-T7451.

II. EXPERIMENTAL PROCEDURES

A. *Materials*

Alloys selected for evaluation were 50-mm-thick 7050-T7451 (2.3Cu-6.2Zn-0.12Si-0-2.3Mg-Al) and 25-mm-thick 6061-T6 (0.6Si-0.7Fe-0.25Cu-0.15Mn-1.0Mg-0.2Cr-0.25Zn-Al). The 7050 Al alloy was selected as a high-strength, non-weldable Al-Cu-Zn alloy of particular interest for aircraft applications; the moderate-strength, weldable 6061 Al alloy was selected both because of its versatility and because it is a commonly used Al alloy.

B. *The FSP Method*

The FSP method locally anneals and creates a fully recrystallized, fine-grained microstructure at selected areas within a thick aluminum plate, thus producing a targeted region with low flow stress and enhanced formability. The FSP tool consisted of a 25-mm-diameter concave shoulder and an 8-mm-diameter cylindrical pin operating at a tilt of 2.8 deg. The plates used for this study were processed using a linear raster pattern, with a tool translation of 3.3 mm per pass; the tool was moved 3.3 mm toward the unprocessed material after the completion of each pass. This approach ensured that the material was fully processed. The raster was continuous such that the travel speed was maintained as the FSP tool reversed direction. For the 25-mm-thick 6061, the processing parameters included a tool rotation rate of 600 rpm, a travel speed of 100 mm/min, and a processing depth of 3 mm. For the 50-mm-thick 7050, the speed was 350 rpm, the feed rate was 127 mm/min, and the processing depth was 6 mm. In all cases, the processing travel direction was perpendicular to the eventual bend axis of the plate. When the processing travel direction is parallel to the plate bend axis, premature failure occurs.[10]

C. *Thick-Section Forming*

Previous work has demonstrated that FSP can be applied to 2519 Al and that, subsequently, 25-mm-thick plate can be bent at room temperature to high-bend angles.[18] This same approach was used here for both 7050-T7451 and 6061-T6 Al alloys. To form or bend thick plate, a relatively robust punch and die were fabricated, where the punch had a radius of 38 mm. For most bend tests, the FSP tensile surfaces were lightly machined to eliminate tool surface markings. The bending of these plates was performed within hours of FSP, to minimize natural aging. Failure of the plates was assumed to occur at the onset of visual crack formation on the tensile surface.

D. *Tension Testing*

To characterize the flow stress gradient that exists through the thickness of a friction-stir-processed plate, tensile specimens were machined from the processed plates at various depths through the thickness. In all cases, the specimens were oriented so that the major strain axis was aligned with the direction in which the processing tool was traveling. The specimens were fabricated using the ASTM E8 standard and testing was performed at a constant rate of 2.54 mm/min.

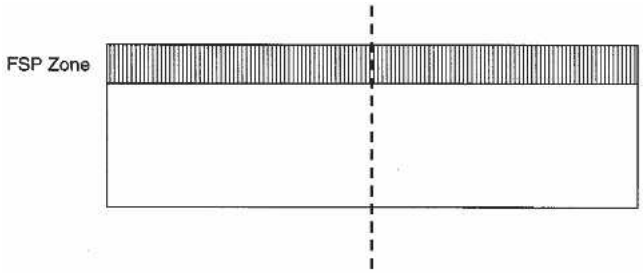

Fig. 1—Microhardness measurements were taken across the thickness of the friction-stir-processed plates, as shown. Most of the softening occurs in the FSP zone, but there is also softening in the base material near the FSP zone, where heat is sufficient to cause aging of heat-treatable aluminum alloys like 6061 and 7050.

E. *Microhardness Testing*

Vickers microhardness testing was done across the thicknesses of both the 6061 and 7050 plates, as shown schematically in Figure 1. The samples were polished in steps, from 320-grit paper to 0.5-μm diamond paste. Tests were performed using an 8-second dwell at 100 g.

III. FINITE ELEMENT ANALYSIS

A. *Model Description*

For a given required bend angle, it would be beneficial to minimize FSP penetration to both reduce processing time *via* higher travel speeds and to reduce heat input, to minimize overaging in the bulk of the structure. This is one of the motivations for developing a predictive model capable of evaluating different processing conditions and their effect on bending performance.

The FORGE2* finite element software[19] was used to develop the plate-bending model. Several key points guided the model development, as follows.

*FORGE2 is a trademark of Transvalor SA, Sophia-Antipolis, France.

(a) Most plate-bending applications are cases of plane-strain or near-plane-strain deformation. Therefore, the plane-strain assumption can be employed. This is simpler and quicker than a three-dimensional simulation.
(b) The model must accurately represent the composite-type properties of a plate that has been processed on one side.
(c) The forming is done at room temperature and, therefore, the elastic component of deformation should not be neglected.
(d) A failure criterion must be used to predict bending limits.

These requirements led to the development of a model using an elastoplastic material law. With this law, springback and, eventually, residual stresses can be predicted; however, in the present effort, the focus is on bending ductility, not residual stresses. Some experimental work on residual stresses in FSW has been done by other authors.[20,21] To account for the composite properties of the plate, the plate

mesh was divided into different zones. The elements in each zone had the average properties of the volume of material represented by that zone. In the simplest case, a plate can be divided into two zones, *i.e.*, one for the base material and another for the friction-stir-processed material, as shown in Figure 2. In more complex cases, a series of zones can be used to represent a gradient of properties through the plate thickness. The model input parameters include the number and size of the zone to be modeled and the stress-strain behavior of each zone.

B. *Failure Criteria*

Two failure criteria have been used to predict bending limits. One is the Latham and Cockroft criterion,[22] designed to predict failure in tension, as shown here:

$$\int_0^{\varepsilon_f} \sigma^* d\varepsilon = C \qquad [1]$$

The critical stress σ^* is the maximum principle tensile stress, calculated as follows:

$$\sigma_{\max} = \frac{\sigma_x + \sigma_y}{2} + \sqrt{\left(\frac{\sigma_x - \sigma_y}{2}\right)^2 + \tau_{xy}^2} \qquad [2]$$

At each increment of the simulation, the failure criterion is evaluated for all elements in the mesh. If a critical value of the criterion is exceeded, then failure is assumed to have occurred. This critical value can be found experimentally by calculating the area under the true stress-true strain tensile curve, for each distinct layer of material used to create the model. Therefore, the critical values are different for each layer of material.

A second method for predicting bending failure uses the von Mises criterion.[23] The expression for effective strain is given as follows:

$$\bar{\varepsilon} = \sqrt{\frac{2}{3}\left(\varepsilon_1^2 + \varepsilon_2^2 + \varepsilon_3^2\right)} \qquad [3]$$

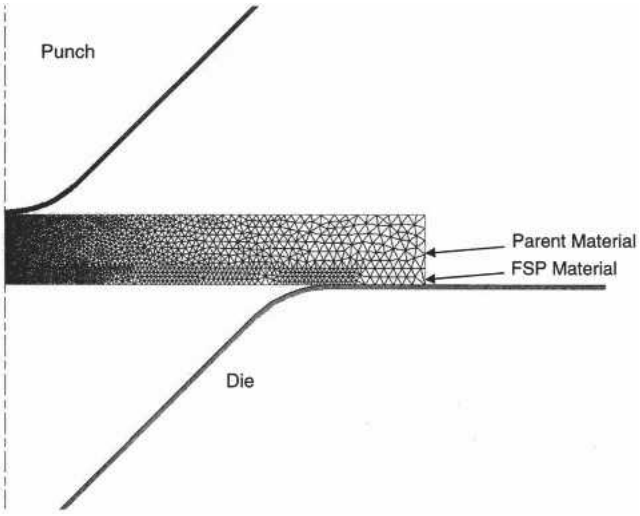

Fig. 2—The finite-element mesh for the plate is divided into two zones, representing different material behaviors: the bottom 3-mm layer has the behavior of the FSP material, while the top 22-mm layer is modeled as the base material. By symmetry, only half of the plate was modeled.

Using the plane-strain condition and the incompressibility relationship, the following expressions are obtained:

$$\varepsilon_2 = 0 \qquad [4]$$

$$\varepsilon_1 + \varepsilon_2 + \varepsilon_3 = 0 \qquad [5]$$

$$\varepsilon_1 = -\varepsilon_3 \qquad [6]$$

Inserting Eq. [6] as a substitute for the expression for the von Mises effective strain (Eq. [3]) results in a relationship between the limit strain in plane strain and the limit strain in uniaxial tension:

$$\varepsilon_1^{PS} = \frac{\sqrt{3}}{2}\,\bar{\varepsilon} \qquad [7]$$

This relation predicts that when plane-strain tension is the mode of deformation, the limit strain will be only 87 pct of that possible in uniaxial tension. For example, when the maximum simulated tensile strain on the outer edge of the plate reaches 87 pct of the failure strain obtained experimentally in a uniaxial tension test, then failure is predicted to have occurred on the plate surface.

IV. RESULTS AND DISCUSSION

A. *The 6061-T6 Aluminum*

Bending experiments were performed on as-received plate and on friction-stir-processed plates. For the 25-mm-thick 6061-T6 plate, approximately 230-mm wide, the as-received plate failed at a bend angle of about 25 deg, while the friction-stir-processed plate failed at approximately an 80-deg bend angle, as seen in Figure 3. Deformation on the plate surface was very close to plane strain, with minor strain of 1 pct or less in the center of the plates on the crown. The increased ductility in the processed plate is due primarily to a decrease in hardness in the outer layer of material that results from the heat of processing. This is seen in the microhardness plot shown in Figure 4. The transition between the

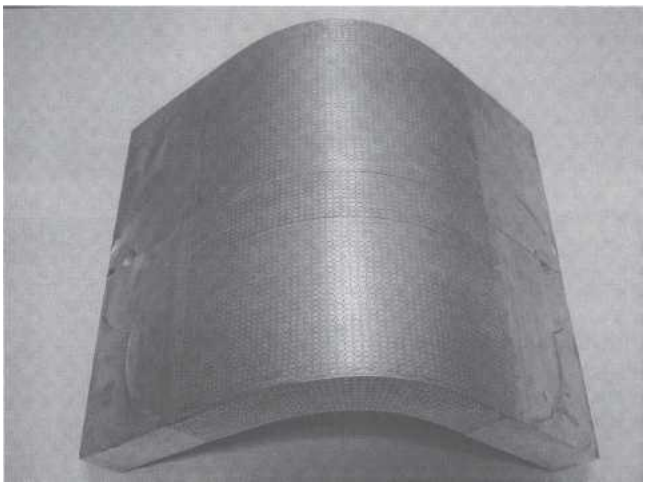

Fig. 3—1-in.-thick 6061-T6 bent to an angle of approximately 80 deg, before cracks began to form on the outer surface. Circle-grid analysis of the surface strains showed that the negative minor strain at the crown was less than 1 pct.

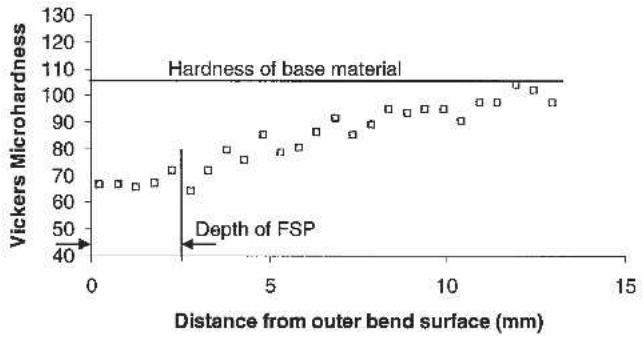

Fig. 4—Hardness profile for 1-in. friction-stir-processed 6061-T6. The hardness in the 3-mm-deep processed zone is uniform, but then gradually increases through the thickness of the plate, until the base metal hardness is reached.

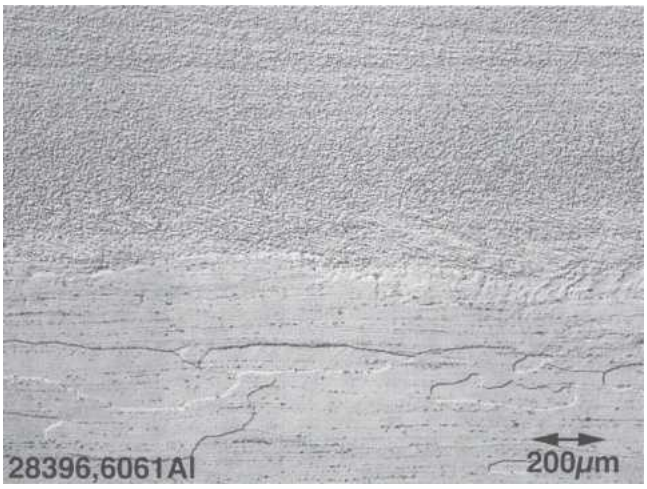

Fig. 5—Micrograph of friction-stir-processed 6061-T6. The transition from the fine-grained microstructure produced by stirring into the unstirred zone is clearly evident. This view is taken from the bottom of the weld nugget, at a depth of approximately 3 mm from the plate surface.

stirred zone and the adjacent unstirred zone is shown in Figure 5, where the stirred zone clearly has very fine grains (1 to 5 μm), compared to the unprocessed base material. The depth of the stirred zone was approximately 3 mm, in this case; the original depth was closer to 5 mm, but the top layer of the material was milled off to provide a smooth surface.

Tension testing was done to obtain stress-strain curves to use as inputs to the model. Specimens were machined from a 1-in.-thick plate that had been processed to a depth of 5 mm, so that the gage section of the reduced E8 specimens, which were 4-mm thick, would consist entirely of processed material. The specimens from the FSP zone, as well as the specimens machined from unprocessed plate, provided the stress-strain curves as inputs to the model, as seen in Figure 6. The mesh was composed of 1146 nodes (2084 linear triangular elements), the punch descended at a rate of 1 mm/s, and the friction coefficient was 0.2.

For the as-received plate, the model predicted a bend angle of about 21 deg, which was close to the experimental result of about 20 deg. This prediction was the same for both the Latham and Cockroft and the von Mises criteria. The pre-

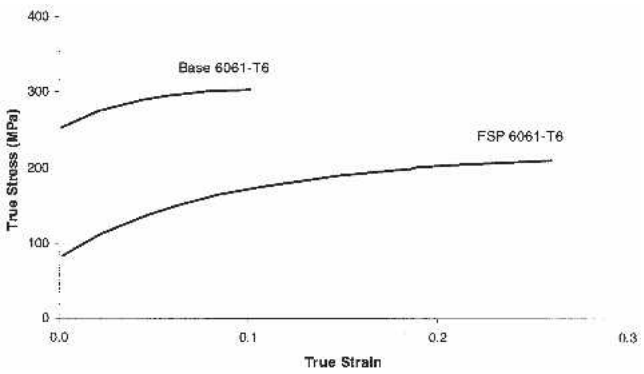

Fig. 6—True stress-true strain tensile curves for base 6061-T6 and friction-stir-processed 6061-T6 (a 5-mm depth of processing). The area under the base material curve is 29 MPa, while the area under the FSP material curve is 45 MPa.

cise angle of the onset of failure in the experiment is not easy to identify, because the bending tests must be interrupted regularly so that the tensile surface of the plate can be inspected for cracks. The agreement is not as good for the friction-stir-processed plate. In this case, the Latham and Cockroft criterion predicts failure at about 62 deg, while the von Mises criterion predicts failure at 75 deg, compared to an experimental result of about 80 deg. The reason for the less accurate prediction lies in the model itself, in which only two distinct zones of material behavior were used to model the plate: one zone consisted of a 3-mm layer of friction-stir-processed material, and an adjacent zone consisted of 22 mm of base material. Since softening occurs much deeper than the processing depth of 3 mm used in the model, (Figure 4), a more precise description of the hardness gradient through the thickness of the plate was needed, in order to produce accurate bending-limit predictions. The next example, on 7050 aluminum, demonstrates a more accurate approach.

B. *The 7050-T7451 Aluminum*

A second trial was performed with 50-mm-thick 7050-T7451 aluminum, in which the plate was friction-stir processed to a depth of 6 mm. The hardness profile for the processed plate is shown in Figure 7 and the microstructure is shown in Figure 8, in which the transition between the fine-grained processed material and the base material occurs at a depth of approximately 6 mm. In order to account for the hardness gradient in the model, a series of tensile specimens were cut from different depths of the friction-stir-processed plate. Twelve tensile specimens, each one about 4-mm thick, were machined from the plate through its thickness, as shown schematically in Figure 9. The tensile curves produced by the 12 specimens are shown in Figure 10. The first four layers of material on the processed side have lower yield and tensile strengths than do the layers through the remainder of the plate. These results correspond well with the hardness curve in Figure 7. A model was constructed using all 12 layers of stress-strain behavior. The undeformed mesh and tooling profiles are shown in Figure 11(a). The plate mesh had 2766 nodes (5343 linear triangular elements), the punch speed was 1 mm/s, and the friction coefficient was 0.2. For this alloy and gradient of properties, the model predicted a bending limit of 20 deg, after springback, for both

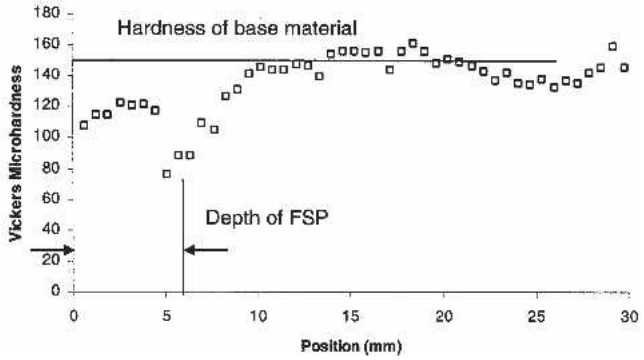

Fig. 7—Microhardness profile across the thickness of 50-mm-thick friction-stir-processed 7050 plate. The plate was processed to a depth of 6 mm, but the heat from processing clearly caused softening deeper into the plate.

Fig. 8—Micrograph of friction-stir-processed 7050-T7451. The transition from the fine-grained microstructure produced by stirring into the unstirred zone is clearly evident.

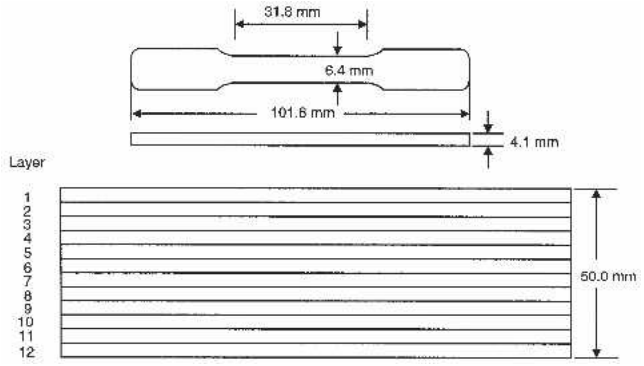

Fig. 9—Schematic of how tension specimens were cut from the 7050 plate. Each specimen was about 4.1-mm thick, so 12 specimens were cut through the thickness of the friction-stir-processed plate. These specimens allowed for characterization of the stress-strain behavior of the plate after processing, where softening occurred well beyond the depth of the processing tool. The major strain axis of the specimen is aligned with the travel direction of the tool.

the von Mises and the Latham and Cockroft criteria. This does not mean that a catastrophic failure would occur at this bend angle, but it does indicate that cracks start to form on the outer

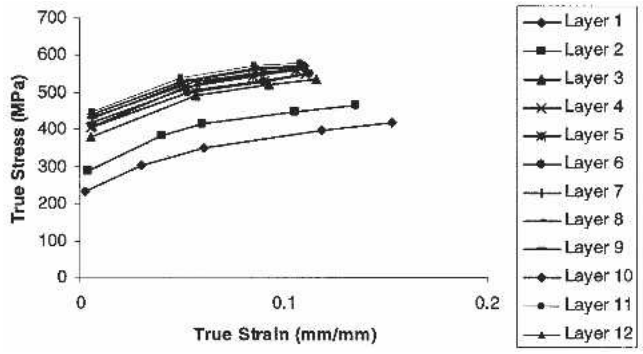

Fig. 10—True stress-true strain tensile curves for layers taken through the thickness of a 50-mm-thick 7075 friction-stir-processed plate. Layer 1 consists entirely of friction-stir-processed material, while Layer 12 is on the opposite side of the plate. The area under the curve for Layer 1 is 58 MPa, and the areas under the other curves decrease more or less uniformly to about 54 MPa in Layer 12.

surface of the plate. This result agrees well with the experiment in which the sample failed at a bending limit of approximately 18 deg. It is encouraging that both failure criteria predict the same bending limit in this case, in which an accurate description of stress-strain behavior through the entire thickness of the plate was used in the model. Figure 11(b) shows the deformed mesh of the plate after springback at the predicted bending limit of 20 deg.

V. SUMMARY AND CONCLUSIONS

The FSP method was used to locally modify the ductility of 6061-T6 and 7075-T7451 aluminum plates. This technique softened the plates both in the processed zone and somewhat beyond the processed zone, resulting in much greater bending limits than were found in the unprocessed base material. A finite-element model was developed, to predict the bending limits of both the base plates and the friction-stir-processed plates. The model employs a mesh with a gradient of stress-strain properties through the thickness, capturing the effect of the FSP of the heat-treatable aluminum alloys. The Latham and Cockroft and the von Mises criteria were used to predict failure, or the onset of cracking, during bending. Both criteria accurately predicted the bending limit of a 25-mm-thick, homogeneous, unprocessed 6061 aluminum plate. However, the prediction of the bending limit of a 25-mm-thick 6061 aluminum plate, having undergone FSP to a depth of 3 mm, was only moderately successful. This is probably because the gradient of properties caused by processing was not accurately taken into account by the model. For this example, the model assumed only two distinct stress-strain behaviors, corresponding to a processed zone and an unaffected base-material zone. In reality, there was a gradient of properties through the thickness of the plate. In this same case, the von Mises criterion predicted a bending limit of 75 deg, and the Latham and Cockroft criterion predicted failure at 62 deg, while the experimentally determined limit was >80 deg. Another trial was performed on 50-mm-thick 7050 aluminum; this time, however, a series of tensile specimens were machined from the thickness of the friction-stir-processed plate, establishing the entire gradient of stress-strain behavior. This resulted

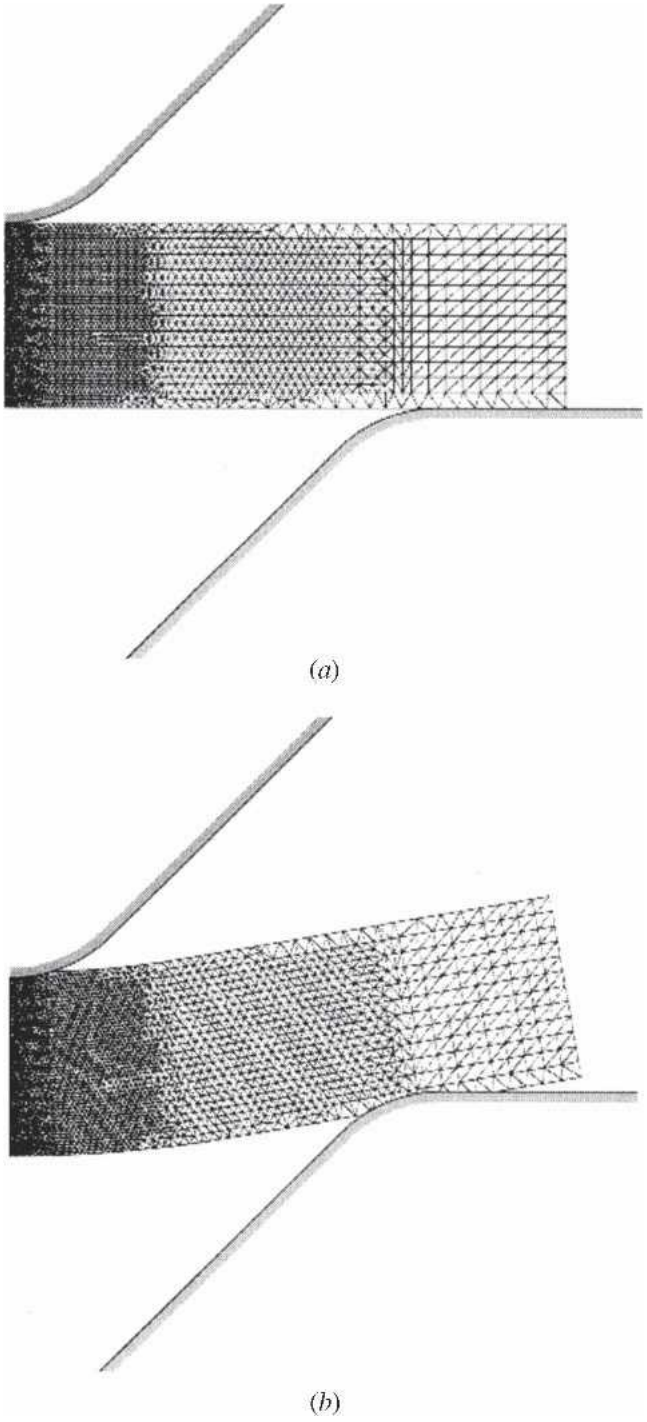

Fig. 11—(*a*) Undeformed configuration of tooling and 50-mm-thick 7050 plate and (*b*) plate bent to 20 deg (including springback), where the model predicts onset of cracking on the outer surface of the plate at this bend angle. By symmetry, only half of the plate was modeled.

in an improved model prediction, with both the Latham and Cockroft and the von Mises criteria predicting a bending limit of 20 deg, compared to an experimentally determined bending limit of about 18 deg.

ACKNOWLEGMENTS

The authors acknowledge DARPA for supporting this work, under contract No. MDA972-02-0030. This document is approved for Public Release, Distribution Unlimited.

REFERENCES

1. S.P. Lynch, D.P. Edwards, A. Majumdar, S. Moutsos, and M.W. Mahoney: *Mater. Sci. Forum*, 2003, vols. 426–432, pp. 2903-08.
2. M. Mahoney, A.J. Barnes, W.H. Bingel, and C. Fuller: *Mater. Sci. Forum*, 2004, vol. 447–448, pp. 505-12.
3. M.W. Mahoney, W.H. Bingel, S.R. Sharma, and R.S. Mishra: *Mater. Sci. Forum*, 2003, vols. 426–432, pp. 2843-48.
4. Z.Y. Ma, R. Mishra, and M. Mahoney: *Scripta Mater*., 2004, vol. 50 (7), pp. 931-35.
5. C. Fuller, M. Mahoney, and W. Bingel: *Proc. 4th Int. Symp. Friction Stir Welding*, Park City, UT, May 2003, TWI Ltd., Cambridge, United Kingdom, 2003.
6. M. Mahoney, R. Mishra, T. Nelson, J. Flintoff, R. Islamgaliev, and Y. Hovansky: *Friction Stir Welding and Processing*, TMS, Warrendale, PA, 2001, pp. 183-94.
7. Z.Y. Ma, R.S. Mishra, M.W. Mahoney, and R. Grimes: *Mater. Sci. Eng*., 2003, vol. A351, p. 148.
8. C. Fuller, M. Mahoney, and W. Bingel: *Proc. 5th Int. Symp. on Friction Stir Welding*, Metz, France, Sept. 2004, TWI Ltd., Cambridge, United Kingdom, 2004.
9. Z.Y Ma, S.R. Sharma, R.S. Mishra, and M.W. Mahoney: *Mater. Sci. Forum*, 2003, vols. 426–432, pp. 2891-96.
10. M. Mahoney, C.B. Fuller, and W.H. Bingel: Rockwell Scientific Co., Thousand Oaks, CA, unpublished research, 2002.
11. Z. Feng, J.E. Gould, and T.J. Lienert: *Hot Deformation of Aluminum Alloys II*, 1998, pp. 149-58.
12. Y.J. Chao, X. Qi, and W. Tang: *J. Manufacturing Sci. Eng*., 2003, vol. 125 (1), pp. 138-45.
13. M. Song and R. Kovacevic: *Int. J. Mach. Tools Manufacture*, 2003, vol. 43, pp. 605-15.
14. C.M. Chen and R. Kovacevic: *Int. J. Mach. Tools Manufacture*, 2003, vol. 43, pp. 1319-26.
15. S. Xu, X. Deng, A.P. Reynolds, and T.U. Seidel: *Sci. Technol. Welding Joining*, 2001, vol. 6, pp. 191-93.
16. P.A. Colegrove and H.R. Shercliff: *Sci. Technol. Welding Joining*, 2003, vol. 8, pp. 360-68.
17. A. Askari, S. Silling, B. London, and M. Mahoney: *Modeling and Analysis of Friction Stir Welding Processes*, TMS, Warrendale, PA, 2001.
18. M. Miles, M. Mahoney, T. Nelson, and R. Mishra: *Friction Stir Welding and Processing II*, TMS, Warrendale, PA, 2003, pp. 253-58.
19. FORGE2, Transvalor SA, Sophia-Antipolis, France.
20. C.D. Donne, G. Biallas, T. Ghinidini, and G. Raimbeaux: *Proc. 2nd Int. Symp. on Friction Stir Welding*, Gothenburg, Sweden, June 26–28, 2000.
21. M.A. Sutton, A.P. Reynolds, D.Q. Wang, and C.R. Hubbard: *J. Eng. Mater. Technol*., 2002, vol. 124 (4), pp. 215-21.
22. M.G. Cockroft and D.J. Latham: *J. Inst. Met*., 1968, vol. 96, pp. 33-39.
23. D.A. Barlow: *J. Mech. Phys. Solids*, 1954, vol. 2, pp. 259-64.